Enhancing trigger sensitivity of nanocarriers through organocatalytic oxidant activation

Piergentili, Irene; Cai, Mao; Klemm, Benjamin; Xu, Bing; Luo, Sanzhong; Eelkema, Rienk

DOI
10.1016/j.xcrp.2023.101547

Publication date
2023

Document Version
Final published version

Published in
Cell Reports Physical Science

Cell Reports
Physical Science

CellPress
OPEN ACCESS

Article

Enhancing trigger sensitivity of nanocarriers through organocatalytic oxidant activation

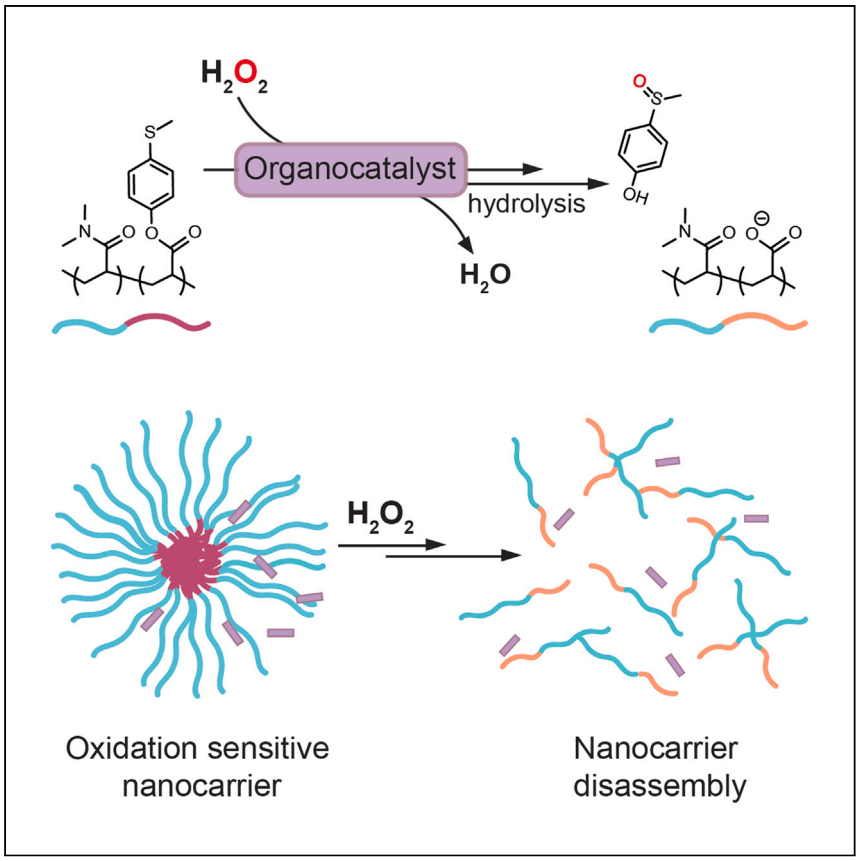

Nanocarriers for targeted delivery often lack sensitivity to biomarker signal concentrations in biological environments. Piergentili et al. report that an imine-based catalyst boosts the response of oxidation-sensitive materials by activating H_2O_2, demonstrating that organocatalysis can improve stimuli amplification and that it enhances controlled delivery system responsiveness.

Irene Piergentili, Mao Cai, Benjamin Klemm, Bing Xu, Sanzhong Luo, Rienk Eelkema

luosz@tsinghua.edu.cn (S.L.)
r.eelkema@tudelft.nl (R.E.)

Highlights

Organocatalysis enhances the sensitivity of nanocarriers to biomarker signals

Efficient conversion of thioether to sulfoxide with H_2O_2 using imine-based catalysts

In situ amino acid-derived imine catalyzes oxidation of thioether-based micelles

Organocatalysis increases nanocarrier disruption rate at low oxidant concentrations

Piergentili et al., Cell Reports Physical Science 4, 101547
September 20, 2023
https://doi.org/10.1016/j.xcrp.2023.101547

Cell Reports
Physical Science

CellPress
OPEN ACCESS

Article

Enhancing trigger sensitivity of nanocarriers through organocatalytic oxidant activation

Irene Piergentili,[1] Mao Cai,[2] Benjamin Klemm,[1] Bing Xu,[3] Sanzhong Luo,[2,*] and Rienk Eelkema[1,4,*]

SUMMARY

The redox balance in tumor and diseased cells often leads to the production of reactive oxygen species (ROS). Many ROS-responsive materials based on sulfur oxidation have been reported with the goal of achieving controlled delivery at the tumor. However, these materials often lack responsiveness to low ROS concentrations present in the tumor environment. To address this, we use organocatalysis to achieve an enhanced response of thioether-based nanocarriers triggered by low concentrations of ROS. Using block copolymer micelles that can disassemble through thioether oxidation followed by ester hydrolysis, this work shows how an *in-situ*-formed imine oxidation catalyst can enhance disassembly kinetics at low millimolar hydrogen peroxide concentrations. The results show that with organocatalysis, Nile Red-loaded micelles release their cargo twice as fast compared to uncatalyzed conditions. This study highlights the potential of organocatalysis as a valuable strategy to enhance the responsiveness of biomarker-triggered delivery systems.

INTRODUCTION

Oxidative stress is an imbalance of the reactive oxygen species (ROS) generated in metabolic pathways.[1–5] Such imbalance can be found in inflamed tissue and the tumor microenvironment. There is a great interest in materials able to respond to oxidative species such as H_2O_2, to target therapeutics to these tissues. Based on this concept, several examples of ROS-responsive materials have been reported, using redox-sensitive elements ranging from sulfur or selenium to boron.[6–12] Building on the work of Hubbel and co-workers on the use of polythioether-based nanocarriers for targeted drug delivery in 2004,[10] the conversion of hydrophobic thioethers to hydrophilic sulfoxide upon reaction with H_2O_2 has been employed extensively to trigger the disassembly of polymeric structures.[13–15] Most of the thioether-bearing systems that have been tested with submillimolar concentrations of H_2O_2 show response times of many days and even weeks to achieve thioether oxidation and nanocarrier destruction, which limits their applicability in biologically relevant conditions (50–100 μM).[16–19] Due to the slow oxidation kinetics of thioethers with H_2O_2, even slightly reducing these timescales, while maintaining material stability and encapsulation efficiency, can be very challenging. Cells commonly use enzymes and enzymatic cascades to amplify these signals by catalytic turnover. Such strategies can be useful to couple targeted drug delivery to the presence of biomarker signals.[20–23] Low-molecular-weight organocatalysts could prove highly useful for this purpose, as they are generally easy to make and use and are often far less toxic than their transition-metal-based counterparts.[24] Still, outside the realm of (enantioselective) synthesis of small-molecule targets, organocatalysis is only sparingly applied, for instance to promote bond formation in polymer synthesis[25–28] or in

[1]Delft University of Technology, Department of Chemical Engineering, Van der Maasweg 9, Delft 2629 HZ, the Netherlands

[2]Center of Basic Molecular Science, Department of Chemistry, Tsinghua University, Beijing 100084, China

[3]Delft University of Technology, Department of Radiation Science and Technology, Mekelweg 15, Delft 2629 JB, the Netherlands

[4]Lead contact

*Correspondence: luosz@tsinghua.edu.cn (S.L.), r.eelkema@tudelft.nl (R.E.)

https://doi.org/10.1016/j.xcrp.2023.101547

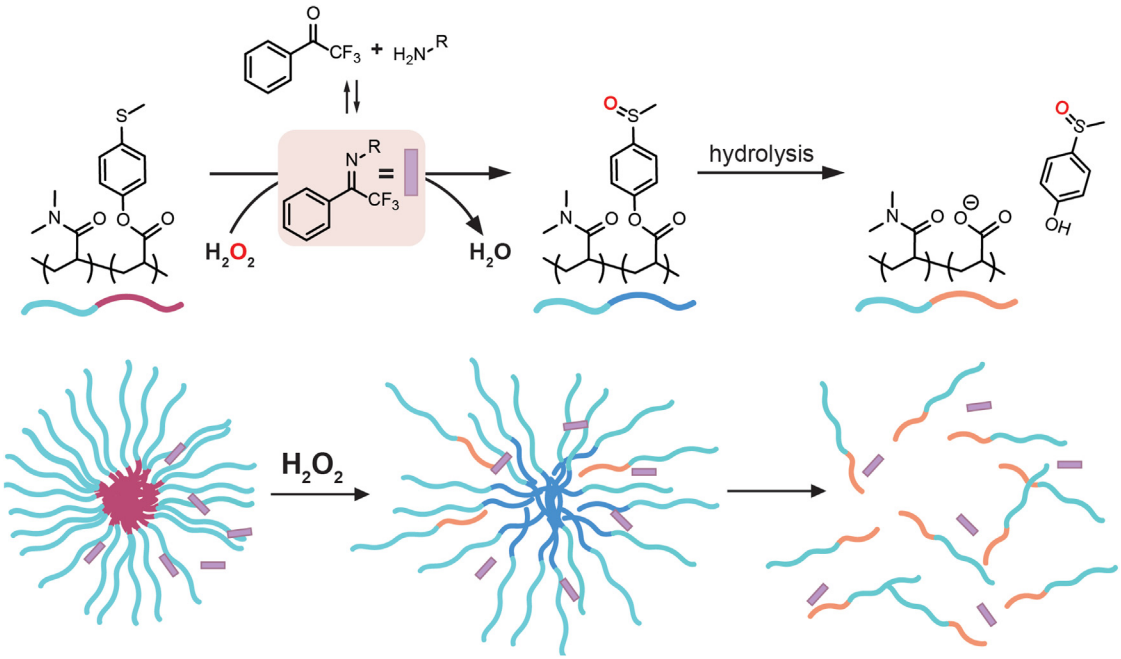

Figure 1. General concept of *in situ* imine formation used to catalyze the oxidation of PM16 micelles with H_2O_2

The conversion of thioether moieties to sulfoxides triggers the hydrolysis of the hydrophobic domain of the amphiphilic polymer, leading to disassembly of the micelles.

dynamic covalent networks.[29,30] Here, we propose the use of organocatalysis to increase the sensitivity of nanocarriers to ROS, enabling sulfur functionalized surfactants to respond to low concentrations of H_2O_2 at reduced timescales.[31,32] Despite many successful examples of organocatalysis to accelerate the oxidation of small-molecule thioethers with H_2O_2,[33–37] application of organocatalysis to augment nanocarrier response has been greatly overlooked.

We recently reported block copolymer micelles that are able to degrade in the presence of H_2O_2 through the oxidation-triggered hydrolysis of their thioanisole-ester-based micellar core.[38] The conversion of a thioether into a more electron-withdrawing group such as a sulfoxide triggers the hydrolysis of the adjacent ester, unmasking the acrylate anion on the polymer backbone (Figure 1). This solubility change in aqueous environment leads to the disassembly of the micelles. This logic gate behavior enables the use of these micelles as nanocarriers for targeted delivery and release systems. In this oxidation-hydrolysis cascade, the slow oxidation[39] is the rate-limiting step. For this reason, high concentrations of H_2O_2 are needed to achieve a material response on an hour timescale.[40] We found that these micelles fully disintegrate within 2 h when elevated concentrations of H_2O_2 (600 mM) were used. This timescale extended to 168 h for 2 mM H_2O_2 (2.2 equiv relative to the estimated thioether units on the polymer). Similar to other thioether-based nanocarrier systems, such high concentrations of H_2O_2 have limited clinical relevance, posing an incentive to develop methods that will allow the acceleration of thioether oxidation at lower concentration.

In the context of enhancing the response of ROS-triggered nanocarriers, we found the prospect of using a simple organocatalyst highly appealing. For this purpose, we had to develop an organocatalyst for the oxidation of thioethers with hydrogen peroxide. In the 1950s, Emmons studied the synthesis and stability of oxaziridines as

an alternative to organic peroxides,[41] and subsequently, many other researchers started to employ this oxidant as a catalyst in sulfoxidations.[42–45] In 1994, the Page group reported the oxidation of alkyl aryl sulfides, using a stoichiometric amount of imine to activate H_2O_2.[46] The need of extra activating agents or bases for *in situ* generation of oxaziridine in these methods discouraged its application for oxidation under mild conditions.[47] Still, based on previous work from our group,[48] we chose to investigate a synthetic two-component imine catalyst that spontaneously forms from a mixture of $PhCOCF_3$ and primary amines. $PhCOCF_3$ can form an imine by reaction with amines, activating H_2O_2, likely through an oxaziridine-like intermediate. This species is more electrophilic than H_2O_2 alone due to the electron-withdrawing ketone, and it is effective even in neutral conditions, which will be important for use in biological environments. We considered the use of water-soluble amines to increase the solubility of the hydrophobic $PhCOCF_3$. The latter was found to be the most promising ketone for the imine formation due to the strongly electron-withdrawing CF_3 group. We included -*t*Bu functionalized amines in our study considering that the presence of *tert*-butyl groups adjacent to the nitrogen was shown to be important to ensure heterocycle stability.[41]

Based on these considerations, we here present a cooperative ketone/amine catalysis to oxidize the thioether-based hydrophobic block of block copolymer surfactants in the presence of H_2O_2 (Figure 1), leading to improved micelle disassembly rates. This approach constitutes a step forward to obtain oxidation-triggered drug-delivery and -release systems able to respond to H_2O_2 levels approaching the concentrations produced in tumors and diseased tissue.

RESULTS AND DISCUSSION

Screening of ketone/amine catalysis for the oxidation of thioether ester molecular model

Based on its efficient α-hydroxylation of β-ketocarbonyls,[48] we investigated combined ketone/amine catalysis to activate H_2O_2 for thioether oxidation. We first chose 4-(methylthio)phenyl acetate **1** (Figure 2A) as a molecular model of the ROS-responsive moiety of the thioanisole-ester-based block copolymer micelles. We then screened conditions for the oxidation of **1** with 1.5 equiv H_2O_2 using different catalysts and solvents (Figure 2C). $PhCOCF_3$ (**3**) was selected as ketone catalyst because of its strongly electrophilic carbonyl group and its proven catalytic activity toward thioether oxidation.[49] Our experiments showed that ketone **3** was indeed fundamental to achieve the oxidation of **1** into the corresponding sulfoxide **2** (Figure 2C, entries 2 and 3). When **3** was used with amine **A1** as the catalytic system in the oxidation of **1** with H_2O_2 in *tert*-butanol (^{t}BuOH), we obtained 85% yield of **2** in 3 h (Figure 2C, entry 1). Under the same conditions, substituting **A1** with **A2** or **A3** led to yields of 65% (Figure 2C, entry 6) and 71% (Figure 2C, entry 7), respectively. Entries 8–11 report a decrease in the yields of **2** when the oxidation of **1** with H_2O_2 in the presence of **3**/**A1** was carried in other solvents. The effect of the solvent can indeed be decisive in sulfoxidation reactions,[50] and ^{t}BuOH provided the best outcome in our case. The use of 2 equiv H_2O_2 in the standard conditions afforded only 47% yield of **2**, caused by substantial overoxidation to the corresponding sulfone. The oxidation to sulfone of the thioether units on the block copolymer would possibly accelerate the hydrolysis of the ester and, consequently, the ROS-triggered micellar disassembly. However, our ultimate objective is to achieve a response of thioanisole-ester-based micelles to very low H_2O_2 concentrations; therefore, increasing the ratio of H_2O_2 to thioether was considered counterproductive to the aim of this work.

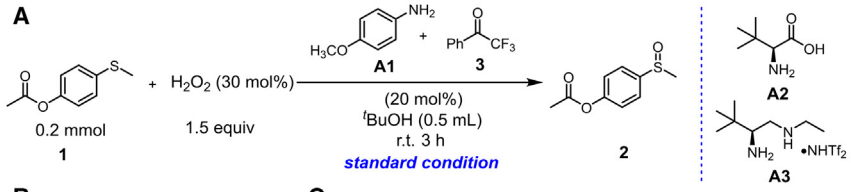

Entry	Variations from standard conditions[a]	Yield[b] (%)
1	none	85
2	without **3**	n.r.
3	acetone instead of **3**	n.r.
4	without H_2O_2	n.r.
5	without amine **A1**	20
6	**A2** instead of **A1**[c]	65
7	**A3** instead of **A1**[c]	71
8	PhMe/DCE instead of ^{t}BuOH	54
9	HFIP instead of ^{t}BuOH	73
10	EtOH/MeOH (4:1) instead of ^{t}BuOH	65
11	3 mL ^{t}BuOH[d]	80
12	2 equiv. of H_2O_2	47

Figure 2. Screening of ketone/amine catalysis for the oxidation of a thioether ester model substrate

(A) Left: scheme of the standard reaction conditions used to test ketone/amine catalysis on the oxidation of 4-(methylthio)phenyl acetate **1**. Right: additional amino catalysts used in the study.

(B) Kinetic order plots for: standard condition (orange ▲), standard condition with the addition of 0.5 mL buffer (0.1 M PBS [pH = 6.95]) (blue ●), and standard condition without the addition of **3** (red ■).

(C) Obtained yield of **2** varying the standard condition.

[a]Reactions were performed with **1** (0.2 mmol), **A1** (20 mol %), **3** (20 mol %), and H_2O_2 (30 wt %, 0.3 mmol) in 0.5 mL ^{t}BuOH at room temperature in air for 3 h.

[b]The yield was determined by GC analysis using n-dodecane as an internal standard (n.r., no reaction).

[c]The reactions were performed in toluene/dichloroethane (v/v 1:1).

[d]The reaction was conducted for 8 h.

Once we confirmed that the standard conditions provide the best performance for the oxidation of **1**, we pursued following the consumption of **1** by gas chromatography (GC) (Figure 2B, orange) over time. We found that the reaction reached completion after 5 h. This result was similar when 0.5 mL buffer (0.1 M phosphate-buffered saline [PBS] [pH = 6.95]) was added (Figure 2B, blue), demonstrating that the presence of aqueous buffer does affect the oxidation kinetics. In contrast, the absence of **3** drastically decreased the rate of sulfoxidation (Figure 2B, red), meaning that the presence of the ketone was fundamental to our system.

Despite the superior results obtained for the sulfoxidation of **1** using **A1** as amino catalyst, the acute toxicity of *p*-anisidine **A1** discouraged us from employing it for drug-delivery purposes. Therefore, in the investigation of H_2O_2-induced degradation of block copolymer micelles in the presence of the ketone/amine catalysts, we mainly focused on the use of **A2** and **A3**.

Synthesis and characterization of PM16 micelles

The block copolymer p(DMA_{130}-b-$MTPA_{16}$), abbreviated as PM16, was synthesized via light-initiated reversible addition fragmentation chain transfer (RAFT) polymerization as we previously described.[38] With 4-(methylthio) phenyl acrylate (MTPA) as hydrophobic monomer and N,N-dimethylacrylamide (DMA) as hydrophilic monomer, this amphiphilic polymer formed micelles in sodium phosphate buffer (1 mg/mL in 100 mM PB [pH = 7.4]) with an average hydrodynamic diameter (D_H)

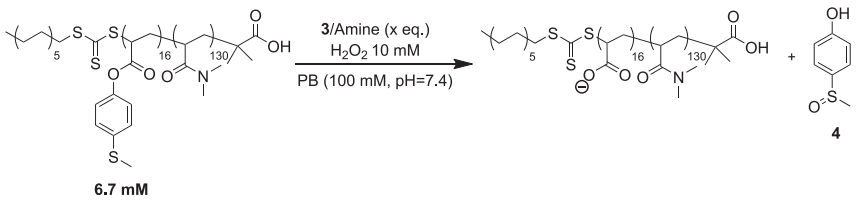

Scheme 1. Ketone/amine catalysis of PM16 block copolymer micelle (6.7 mM thioether units) oxidation by H_2O_2, followed by ester hydrolysis

of 31.6 ± 0.5 nm (Table S1), measured by dynamic light scattering (DLS). A polymer concentration of 8 mg/mL afforded a D_H of 27.3 ± 0.3 nm (Table S1). This slight decrease in PM16 micelle size for higher polymer concentrations is possibly caused by multi-scattering registered by DLS in the presence of a higher number of micelles.[51]

Ketone/amine-catalyzed H_2O_2-induced oxidation and hydrolysis of PM16 micelles

With the micelles and the optimized catalytic conditions in hand, the next step was to study the impact of catalysis on the H_2O_2-induced oxidation and hydrolysis of the thioether ester moieties on PM16. In neutral aqueous media, the formation of the imine catalyst is disfavored over the separate ketone and amine components.[24] Premixing $PhCOCF_3$ and the amine was fundamental to ensure catalytic activity in PM16 oxidation. The solution of **3**/amine using either **A2** or **A3** (0.2, 0.3, and 1 equiv compared to the estimated number of thioether functionalities) was added to PM16 (6.8 mg/mL) in PB/D_2O 9:1 (Scheme 1). After the addition of 10 mM H_2O_2, the reaction was followed at 37°C by ^{1}H nuclear magnetic resonance (NMR) spectroscopy over time. We analyzed process progression through the integration of the sharp aromatic peaks of phenol **4** (Scheme 1; spectra section in the supplemental information), which is the degradation product obtained from the polymer hydrolysis after oxidation.[38]

The addition of 10 mM H_2O_2 to the micelles, in the absence of a catalyst, led to the formation of 94% of **4** in 123 h (Figure 3A). A similar conversion was obtained when 0.2 equiv **3**/**A3** was added with H_2O_2 to the micelles, but now the conversion to **4** reached 50% ($T_{1/2}$) within 25 h against the 39 h necessary without a catalyst present (Figure 3B). Increasing the amount of **3**/**A3** catalyst to 0.3 equiv further reduced the half-life time to 19 h. Using **A2** together with **3** as catalysts in the H_2O_2-triggered oxidation of the micelles led to $T_{1/2}$ of ~17 and 11 h when 0.2 and 0.3 equiv were used, respectively. Interestingly, for these catalytic conditions, we observed sigmoidal profiles of the formation of **4**, meaning that the degradation mechanism mainly follows autocatalytic sulfoxidation and hydrolysis of the PM16 micelles.[38,52,53] The dramatic improvement in the rate of PM16 oxidation and hydrolysis with higher amounts of **3**/**A2** brought us to push the system using 1 equiv of the catalyst mixture. In this case, 96% of **4** formed in 24 h, reaching $T_{1/2}$ in under 7 h (Figure 3B). Thus, with equal H_2O_2 concentrations, PM16 micelles degraded 5.5 times faster with catalysis than in catalyst-free conditions. For all experiments with 0.2–0.3 equiv catalysts, the ^{1}H NMR spectra at t = 0 showed substantially diminished aromatic peaks of **3** (Figures S1 and S2), reaching an estimated integration corresponding to less than 0.1 equiv even when the conversion to **4** was close to 100% at t = 120 h. This observation suggests that **3** is first partially encapsulated in PM16 micelles and then in the residual clusters of the hydrolyzed polymer chains.[38] In contrast, the signals of the **A2** were clearly visible in all the ^{1}H NMR spectra

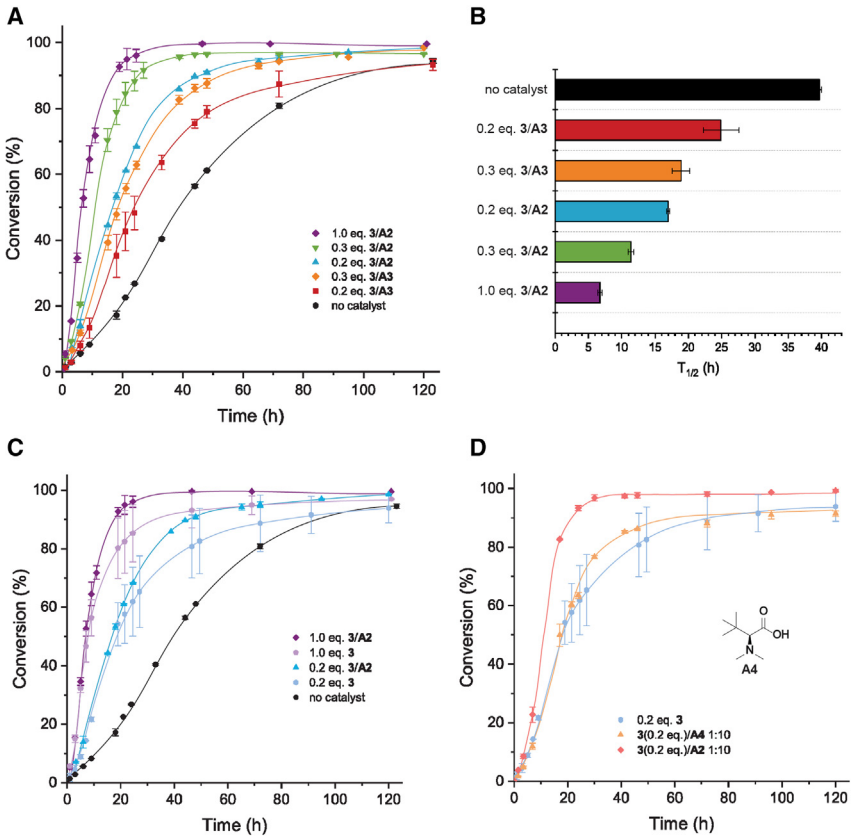

Figure 3. ^{1}H NMR study of ketone/amine catalysis for the oxidation and hydrolysis of thioanisole-ester-based micelles

(A) Conversion measured through ^{1}H NMR spectroscopy of **4** after addition of 10 mM H_2O_2 to PM16 micellar solutions (6.8 mg/mL) in PB (100 mM [pH = 7.4])/D_2O 9:1 at 37°C.

(B) Evaluation of the use of different ketone/amino catalyst conditions based on $T_{1/2}$ of ^{1}H NMR conversion of **4**.

(C) Comparison of the ^{1}H NMR conversion of **4** in presence of 1 and 0.2 equiv **3**/**A2** with 1 and 0.2 equiv **3** in PM16 micelle degradation with 10 mM H_2O_2.

(D) Comparison of the ^{1}H NMR conversion of **4** between the use of 0.2 equiv **3** with an excess of **A2** versus an excess of **A4** (10 equiv with respect to **3**) in PM16 micelle degradation with 10 mM H_2O_2.

All curves are drawn as a guide for the eye. Error bars are the standard deviation of duplicate experiments.

See also Figures S1–S4.

(Figures S2 and S4), confirming that L-*tert*-leucine is well solubilized in the aqueous phase. These observations suggest that the ketone and the amine continuously form enough imine catalyst at the interface of the core and the corona of PM16 micelles to activate the H_2O_2 that surrounds the micelles.

To further investigate the role of the different catalysts into the PM16 micelle oxidation and hydrolysis, we also studied the catalytic effect of having only **3** present (Figure 3C). After the addition of 10 mM H_2O_2 to the micellar dispersions, the $T_{1/2}$ was ~7 and 17 h for, respectively, 1 and 0.2 equiv **3**. Surprisingly, these results were similar to those obtained when mixtures of **3** and **A2** were used as catalyst. However, at roughly around t = $T_{1/2}$, the average conversion decreased compared to the combined use of **3**/**A2**, and large variance was observed for all data close to 90% conversion of **4**. Our interpretation here is that the kinetic profile would be heavily influenced by the scarce solubility of **3** when the micelles gradually disassembled.

H_2O_2 activation by **3** is well known,[49,54,55] but in neutral conditions, the formation of the corresponding dioxirane is considered unfavorable.[55–57] Possibly, $PhCOCF_3$ activates H_2O_2 by forming the corresponding perhydrate. However, this perhydrate is a metastable compound that continuously reverts to $PhCOCF_3$ and H_2O_2.[58] When at $t = T_{1/2}$ more than 0.5 equiv H_2O_2 was consumed, the formation of the perhydrate became progressively less favored. In addition, the first part of the kinetic profile in the presence of 0.2 equiv **3** compares well with that in the presence of 0.3 equiv **3**/**A3** (Figure S3). However, after 24 h, the conversion to **4** slowed down, aligning with the profile obtained with 0.2 equiv **3**/**A3**. For **3**/**A3**, we noticed that the ^{1}H NMR signal at 0.97 ppm (the *tert*-butyl group of **A3**) completely disappeared after 18 h (Figure S1). This observation suggests that **A3** was not present in the system after that time point, resulting in **3** remaining as the only catalytic species. Likely, the nucleophilic secondary amine group of **A3** substituted compound **4** on the ester moiety of the polymer, leading to a decrease of [**A3**] available for catalysis. This undesired effect is prevented by using **A2** because the primary amine is not nucleophilic enough to attack the carbonyl moiety of the ester in neutral conditions.[59] In fact, [**A2**] appeared to be constant over time (Figure S2) under the applied conditions. These observations explain the catalytic superiority of **A2** over **A3** and also the improved control and reproducibility compared to the exclusive use of **3**.

To confirm that **A2** does not act as a phase-transfer catalyst, we synthesized *N*,*N*-dimethyl *tert*-leucine **A4**, a tertiary amine that is not able to form the imine with **3** but may have influence on the solubility of the ketone. In the micellar degradation studies, we chose to have the amine 10 times in excess compared with the ketone to push the imine formation. We conducted these experiments with 0.2 equiv **3** to have the conversion profile of **4** with only 0.2 equiv ketone as reference and, at the same time, to avoid an extreme excess of charged species (both **A2** and **A4**) that could destabilize the micellar system. In Figure 3D, we show how the use of 1:10 **3**/**A4** produced a profile in line with that obtained in the presence of only 0.2 equiv **3**. Here, the use of **A4** led to lower variance in the data. This effect confirms the assumption that once most of the micelles are disassembled, the catalytic activity of the ketone is influenced by its solubility in solution. The oxidation catalyzed by 1:10 **3**/**A2** compared with that in the presence of 0.2 equiv **3** and of 1:10 **3**/**A4** showed almost 2-fold faster formation of **4** as well as higher conversion (98% against 90%–94%). Moreover, with only 0.2 equiv **3** but a large excess of **A2**, we obtained a conversion profile similar to the one with 0.3 equiv 1:1 **3**/**A2**. This dependency on the ratio **3**/**A2** confirms the formation of the imine. Here, despite the fact that the imine formation is disfavored in aqueous environment, an excess of the amine can promote this equilibrium and then activate H_2O_2, likely through an oxaziridine intermediate (Scheme 2).

Morphological study of ketone/amine-catalyzed H_2O_2-induced oxidation and hydrolysis of PM16 micelles

After demonstrating that the cooperative catalysis between the ketone and the amine of H_2O_2 can enhance PM16 micelle oxidation and subsequent hydrolysis, we then pursued studying how this catalytic system would influence morphological change at the material level. To PM16 (6.7 mM thioether units at 6.8 mg/mL polymer concentration) in PB, 0.2 equiv premixed catalyst **3**/**A2** or **3**/**A3** was added. Then, similarly to ^{1}H NMR experiments, 10 mM H_2O_2 was added, and the micelles were analyzed by DLS, following Z-average diameter (Figures S5A, top, and S6, top) and scatter count (Figures S5A, bottom, and S6, bottom) at different time points. In the presence of **3**/**A2** as catalyst, the scatter count of PM16 micelles dropped from 12 to 1.6 Mcps in 48 h, reaching an equilibrium. The Z-average diameter of

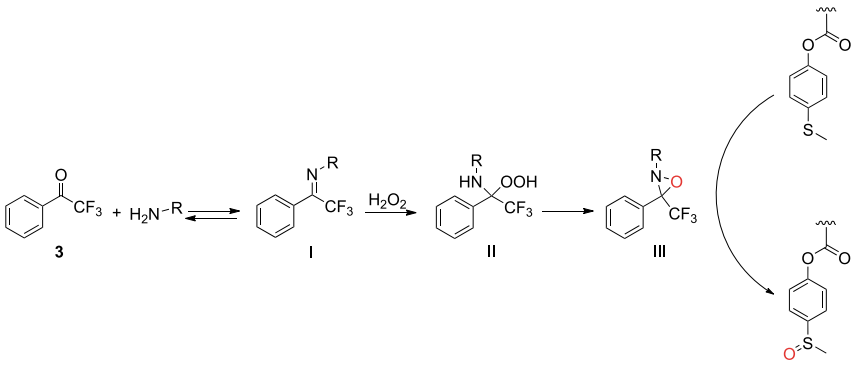

Scheme 2. Proposed catalyst intermediates in ketone/amine-catalyzed oxidation of thioanisole-ester-based block copolymer

Ketone **3** and amine **A2** or **A3** form the imine intermediate I as suggested from the results in Figure 3D. The addition of H_2O_2 leads to the formation of the hydroperoxyamine II (from Page et al.[46]), which can form the oxaziridine III owing to the presence of the strong electron-withdrawing group CF_3 and the stabilization provided by the *tert*-butyl group present in both **A2** and **A3** (from Emmons[41] and Cai et al.[48]).

micelles remained constant during this time but from 48 h onward increased from 31 to 53 nm at 120 h (Figure S5A, ▲ blue line). When **3**/**A3** was employed as catalyst, the minimum scatter count was 2.9 Mcps, and the Z-average diameter increased to 49 nm in 72 h, reaching 78 nm at 120 h (Figure S5A, ■ red line). These results show that the employed catalysis accelerated the H_2O_2-induced PM16 micelle disassembly compared with the control in which no catalyst was used (Figure S5A, ● black line). Interestingly, at the same concentrations of polymer and reactants in the presence of **3**/**A2**, the minimum value in scatter count and the 90% conversion of **4** found in the ^{1}H NMR study were reached at the same time point (44 h) (Figure 4A, ▲ blue line). A similar outcome can be noted for the control experiments at 120 h. This effect confirms that the morphological change in the micellar structure is directly dependent on the ester cleavage into **4** and the acrylate anion. In the DLS data of the micelle degradation in the presence of **3**/**A3**, the fast increase of the Z-average diameter together with the slow decrease in scatter count (Figure S5A, ■ red line) suggests the formation of new amphiphilic structures. This result is in line with ^{1}H NMR evidence and supports our previous hypothesis about the reaction of **A3** with the polymer acrylate esters. In view of this outcome, we chose to use **A2** instead of **A3** as the amine in our catalytic system.

Subsequently, we wanted to test organocatalysis at polymer and H_2O_2 concentrations that are more relevant for drug delivery. We followed the Z-average diameter and scatter count of PM16 micelles at a polymer concentration of 0.9 mg/mL in the presence of 1.3 mM H_2O_2 (1.5 equiv relative to the 0.9 mM thioether units). We observed a 40% decrease of the normalized scatter count under these conditions after 120 h, against the 40 h necessary to achieve the same result for the 8 times more concentrated sample. The Z-average diameter increased from 30 to 43 nm for PM16 micelles at a polymer concentration of 6.8 mg/mL and from 33 to 39 nm for PM16 micelles at a polymer concentration of 0.9 mg/mL at 120 h, showing a minor change in micellar size for both dilution conditions. (Figure S5B). These results demonstrate that 8-fold dilution causes a 3 times decrease in the disintegration kinetics of 1:1.5 PM16/H_2O_2 but a negligible morphological change of the micelles. Knowing this, we pursued applying the optimized catalytic system constituting 1 equiv of **3**/**A2** (Figure 3B) in the diluted conditions. Immediately after adding H_2O_2, the Z-average diameter of PM16 micelles in the presence of the

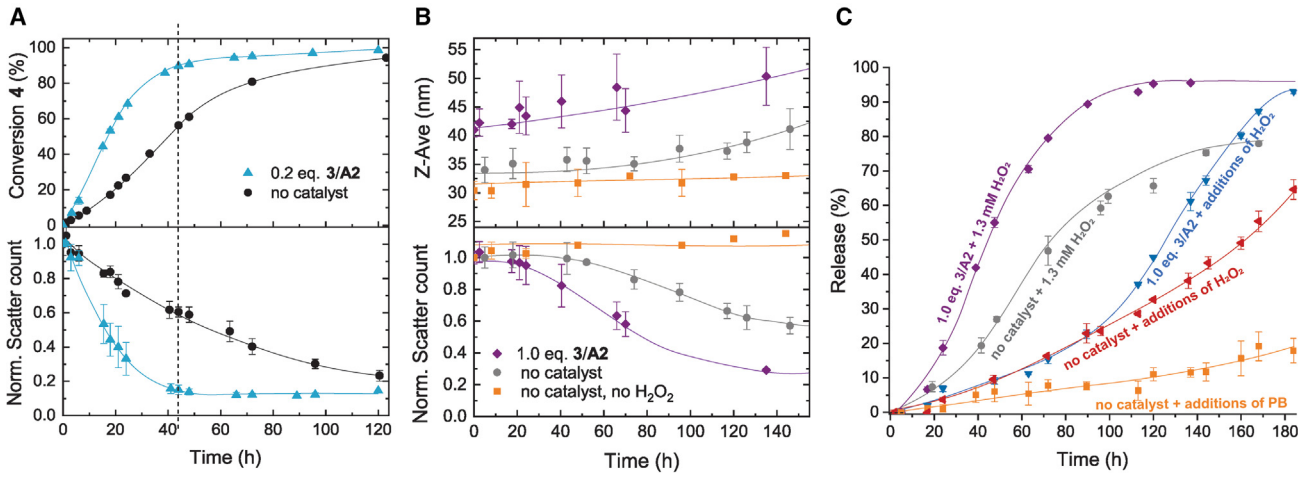

Figure 4. Morphological and cargo release studies of the optimized organocatalytic conditions for the oxidation and hydrolysis of thioanisole-ester-based micelles

(A) Conversion to **4** (%) measured by ^{1}H NMR (top) and normalized scatter count (bottom) measured by DLS of PM16 micelles (6.8 mg/mL) with 0.2 equiv **3/A2** against the control (without any catalyst) after addition of 10 mM H_2O_2 at 37°C. The catalyzed samples reached 90% conversion of **4** and a scatter count plateau value at 44 h (vertical dashed line).

(B) Z-average diameter (top) and scatter count (bottom) of PM16 micelles (0.9 mg/mL) after addition of 1.3 mM H_2O_2 with 1 equiv **3/A2** (◆ purple line) and without catalyst (● gray line). Z-average diameter (top) and scatter count (bottom) of PM16 micelles (0.9 mg/mL) measured by DLS at 37°C (■ orange line).

(C) Nile Red release from PM16 micelles (0.9 mg/mL) after addition of 1.3 mM H_2O_2 with 1 equiv **3/A2** (◆ purple line) and without catalyst (● gray line). Nile Red release from PM16 micelles (0.9 mg/mL) with 1 equiv **3/A2** (▼ blue line) and without catalyst (◄ red line) after continuous addition of 0.5 mM H_2O_2 (24 μL) per day. Nile Red release from PM16 micelles (0.9 mg/mL) after continuous addition of 24 μL PB per day (■ orange line).

The curves are drawn as a guide for the eye. Error bars are the standard deviation of duplicate experiments.

See also Figure S5.

catalyst was 41 ± 1.3 against 33.4 ± 2.9 nm in the absence of catalyst (Figure 4B, top). This size increase of the micelles may be caused by the partial encapsulation of **3**, as anticipated from ^{1}H NMR data. Despite the different starting Z-average diameter, the micellar size change in time showed a similar trend for both catalyzed and non-catalyzed conditions over 140 h (Figure 4B, top). PM16 micelles showed stable values for both Z-average diameter and scatter count in the absence of catalyst and oxidant (Figure 4B, ■ orange line). In the presence of 1 equiv **3/A2** and 1.3 mM H_2O_2, the normalized scatter count showed a more than 40% decrease after about 72 h, while it decreased by barely 20% in the absence of catalyst (Figure 4B, bottom). Therefore, the dissociation of PM16 micelles after H_2O_2 addition proceed two times faster when 1 equiv **3/A2** was employed in diluted conditions. Here, the effect of organocatalysis on the oxidation of thioether moieties of low-concentration PM16 micelles with H_2O_2 is smaller than the 5.5 times increase in rate obtained for the ^{1}H NMR experiment concentrations. Still, despite this dilution-induced effect, the data show that organocatalysis can be applied to increase the rate of nanocarrier disassembly even at very low oxidant concentrations.

Cargo release studies

To study the role of the organocatalytic **3/A2** system for oxidation-triggered release of cargo from PM16 micelles, we loaded PM16 micelles (1 mg/mL) with the hydrophobic dye Nile Red (Figure S7) as previously reported.[38] Then, similarly to the samples measured by DLS, we added 1 equiv **3/A2** and 1.3 mM H_2O_2 to the Nile Red-loaded micelles, and we followed the Nile Red fluorescence over time. Figure 4C shows 80% dye release within 72 h in the presence of organocatalysis against the

168 h necessary in non-catalyzed conditions. In line with the DLS data (Figure 4B), cargo release is approximately twice as fast under catalytic conditions compared with the uncatalyzed scenario.

Finally, we tested the organocatalyzed system under tumor-mimicking conditions, where submillimolar concentrations of oxidant are continuously produced.[32] We used syringe pumps for the addition of 0.5 mM H_2O_2 (24 μL) per day to Nile Red-loaded PM16 micelles (1 mg/mL) with 1 equiv **3**/**A2**. After only 15% release after 72 h, the release reached 90% over the subsequent 90 h (Figure 4C, ▼blue line), similar to the sample in which 1.3 mM H_2O_2 was added directly from the start. The initial delay in release may be due to the initial absence of the catalytically active species, which requires a reaction between the ketone/amine precatalyst and an equivalent of hydrogen peroxide to form (Scheme 2). On the other hand, in the absence of catalyst, the continuous addition of 0.5 mM H_2O_2 (24 μL) per day led to only 55% release at 168 h. When the same volume of PB (■ orange line) was continuously added instead of the H_2O_2 solution, the release profile remained relatively stable over time, reaching less than 20% release after 180 h. This minor passive leakage of Nile Red from PM16 micelles was already noted in our previous work,[38] and it may be slightly increased by the progressive dilution of the micellar dispersions. In the end, in the presence of **3**/**A2**, PM16 micelles showed an about two times faster response to low H_2O_2 concentrations such as 0.5 mM per day compared with the uncatalyzed case and showed good stability in non-oxidative conditions for more than 7 days. Overall, when submillimolar concentrations of H_2O_2 are used, the 2-fold decrease of degradation time for PM16 micelles coupled with the organocatalyst translate to saving several days to achieve the complete cargo release.

In view of these promising results, we performed cytotoxicity assay on PM16 micelles with 1 equiv **3**/**A2** to investigate the potential of this system for biomedical applications. PM16 micelles already showed high cell viability in our previous study,[38] and we found here good cytocompatibility also in the presence of the organocatalyst under the conditions employed for the cargo release experiments (Figure S8).

In this study, we present organocatalytic enhancement of oxidation-triggered disassembly and release from block copolymer micelles, even at very low oxidant concentrations. We applied an *in-situ*-formed imine to catalyze the oxidation of thioether-phenyl-ester-based polymer surfactants in the presence of H_2O_2. Micelles assembled from these surfactants are able to disrupt following a logic gate response in which, after the oxidation of the thioether, the adjacent ester bond cleaves through hydrolysis. The micellar system was doped with the ketone $PhCOCF_3$ **3** and the unnatural amino acid L-*tert*-leucine **A2**. The *in-situ*-formed imine is able to catalytically activate H_2O_2 in aqueous buffer at pH 7.4. The use of organocatalysis on PM16 micelles showed a 5.5-fold acceleration compared with non-catalyzed conditions, at low millimolar concentrations of H_2O_2. In 8 times diluted conditions, Nile Red-loaded micelles in the presence of **3**/**A2** show 80% release more than two times faster than in absence of catalyst. In addition, the same system is able to reach an almost complete release over 7 days when only 0.5 mM H_2O_2 is supplied per day. At the same time, these PM16 micelles show only dilution-induced release over the same time frame in a non-oxidative environment. In addition, the satisfactory cytocompatibility found for this micelle/catalyst system makes **3**/**A2** a promising tool to further enhance the sensitivity of thioether-based platforms that have already an optimized design for biomedical applications.[13] The concept of using organocatalysis for oxidant activation opens the possibility of using the low oxidant concentrations present in living tissues as triggers for bond-breaking reactions and controlled release materials.

EXPERIMENTAL PROCEDURES

Resource availability

Lead contact

Further information and requests for resources and reagents should be directed to the lead contact, Rienk Eelkema (R.Eelkema@tudelft.nl).

Materials availability

All unique/stable reagents generated in this study are available from the lead contact without restriction.

Data and code availability

^{1}H-NMR, DLS, and fluorescence spectroscopy data have been deposited at 4TU.ResearchData :https://doi.org/10.4121/3302580d-ade4-43ce-9d64-61c9583572f4 and are publicly available as of the date of publication.

SUPPLEMENTAL INFORMATION

Supplemental information can be found online at https://doi.org/10.1016/j.xcrp.2023.101547.

ACKNOWLEDGMENTS

The authors acknowledge financial support by the Netherlands Organisation for Scientific Research and the National Natural Science Foundation of China (NWO-NSFC joint project, 21861132003).

AUTHOR CONTRIBUTIONS

I.P., M.C., S.L., and R.E. designed the experiments; I.P. and M.C. synthesized the materials; I.P., M.C., B.K., and B.X. conducted the experiments. I.P. wrote the manuscript, and all authors commented on the work and the manuscript.

DECLARATION OF INTERESTS

The authors declare no competing interests.

INCLUSION AND DIVERSITY

We support inclusive, diverse, and equitable conduct of research.

Received: February 6, 2023
Revised: June 27, 2023
Accepted: July 28, 2023
Published: August 22, 2023

REFERENCES

1. Liou, G.-Y., and Storz, P. (2010). Reactive Oxygen Species in Cancer. Free Radic. Res. *44*, 479–496. https://doi.org/10.3109/10715761003667554.

2. Forrester, S.J., Kikuchi, D.S., Hernandes, M.S., Xu, Q., and Griendling, K.K. (2018). Reactive Oxygen Species in Metabolic and Inflammatory Signaling. Circ. Res. *122*, 877–902. https://doi.org/10.1161/CIRCRESAHA.117.311401.

3. Cheung, E.C., and Vousden, K.H. (2022). The Role of ROS in Tumour Development and Progression. Nat. Rev. Cancer *22*, 280–297. https://doi.org/10.1038/s41568-021-00435-0.

4. Perillo, B., Di Donato, M., Pezone, A., Di Zazzo, E., Giovannelli, P., Galasso, G., Castoria, G., and Migliaccio, A. (2020). ROS in Cancer Therapy: The Bright Side of the Moon. Exp. Mol. Med. *52*, 192–203. https://doi.org/10.1038/s12276-020-0384-2.

5. Casas, A.I., Dao, V.T.-V., Daiber, A., Maghzal, G.J., Di Lisa, F., Kaludercic, N., Leach, S., Cuadrado, A., Jaquet, V., Seredenina, T., et al. (2015). Reactive Oxygen-Related Diseases: Therapeutic Targets and Emerging Clinical Indications. Antioxid. Redox Signal. *23*, 1171–1185. https://doi.org/10.1089/ars.2015.6433.

6. Zhao, C., Chen, J., Zhong, R., Chen, D.S., Shi, J., and Song, J. (2021). Oxidative-Species-Selective Materials for Diagnostic and Therapeutic Applications. Angew. Chem. Int. Ed. *60*, 9804–9827. https://doi.org/10.1002/anie.201915833.

7. Kang, C., Gwon, S., Song, C., Kang, P.M., Park, S.-C., Jeon, J., Hwang, D.W., and Lee, D. (2017). Fibrin-Targeted and H2O2-Responsive Nanoparticles as a Theranostics for Thrombosed Vessels. ACS Nano *11*,

6194–6203. https://doi.org/10.1021/acsnano.7b02308.

8. Ke, W., Li, J., Mohammed, F., Wang, Y., Tou, K., Liu, X., Wen, P., Kinoh, H., Anraku, Y., Chen, H., et al. (2019). Therapeutic Polymersome Nanoreactors with Tumor-Specific Activable Cascade Reactions for Cooperative Cancer Therapy. ACS Nano *13*, 2357–2369. https://doi.org/10.1021/acsnano.8b09082.

9. Wang, S., Yu, G., Wang, Z., Jacobson, O., Lin, L.-S., Yang, W., Deng, H., He, Z., Liu, Y., Chen, Z.-Y., and Chen, X. (2019). Enhanced Antitumor Efficacy by a Cascade of Reactive Oxygen Species Generation and Drug Release. Angew. Chem. Int. Ed. *58*, 14758–14763. https://doi.org/10.1002/anie.201908997.

10. Napoli, A., Valentini, M., Tirelli, N., Müller, M., and Hubbell, J.A. (2004). Oxidation-Responsive Polymeric Vesicles. Nat. Mater. *3*, 183–189. https://doi.org/10.1038/nmat1081.

11. Xu, L., Zhao, M., Gao, W., Yang, Y., Zhang, J., Pu, Y., and He, B. (2019). Polymeric Nanoparticles Responsive to Intracellular ROS for Anticancer Drug Delivery. Colloids Surf., B *181*, 252–260. https://doi.org/10.1016/j.colsurfb.2019.05.064.

12. Yu, L., Zhang, M., Du, F.-S., and Li, Z.-C. (2018). ROS-Responsive Poly(ε-caprolactone) with Pendent Thioether and Selenide Motifs. Polym. Chem. *9*, 3762–3773. https://doi.org/10.1039/C8PY00620B.

13. El Mohtadi, F., d'Arcy, R., Burke, J., Rios De La Rosa, J.M., Gennari, A., Marotta, R., Francini, N., Donno, R., and Tirelli, N. (2020). "Tandem" Nanomedicine Approach against Osteoclastogenesis: Polysulfide Micelles Synergically Scavenge ROS and Release Rapamycin. Biomacromolecules *21*, 305–318. https://doi.org/10.1021/acs.biomac.9b01348.

14. Criado-Gonzalez, M., and Mecerreyes, D. (2022). Thioether-Based ROS Responsive Polymers for Biomedical Applications. J. Mater. Chem. B *10*, 7206–7221. https://doi.org/10.1039/D2TB00615D.

15. Poole, K.M., Nelson, C.E., Joshi, R.V., Martin, J.R., Gupta, M.K., Haws, S.C., Kavanaugh, T.E., Skala, M.C., and Duvall, C.L. (2015). ROS-Responsive Microspheres for on Demand Antioxidant Therapy in a Model of Diabetic Peripheral Arterial Disease. Biomaterials *41*, 166–175. https://doi.org/10.1016/j.biomaterials.2014.11.016.

16. Gupta, M.K., Meyer, T.A., Nelson, C.E., and Duvall, C.L. (2012). Poly(PS-b-DMA) Micelles for Reactive Oxygen Species Triggered Drug Release. J. Control. Release *162*, 591–598. https://doi.org/10.1016/j.jconrel.2012.07.042.

17. Herzberger, J., Fischer, K., Leibig, D., Bros, M., Thiermann, R., and Frey, H. (2016). Oxidation-Responsive and "Clickable" Poly(ethylene glycol) via Copolymerization of 2-(Methylthio) ethyl Glycidyl Ether. J. Am. Chem. Soc. *138*, 9212–9223. https://doi.org/10.1021/jacs.6b04548.

18. Wu, W.-X., Yang, X.-L., Liu, B.-Y., Deng, Q.-F., Xun, M.-M., Wang, N., and Yu, X.-Q. (2016). Lipase-catalyzed Synthesis of Oxidation-Responsive Poly(ethylene glycol)-b-poly(β-thioether ester) Amphiphilic Block Copolymers. RSC Adv. *6*, 11870–11879. https://doi.org/10.1039/C5RA21779B.

19. Halliwell, B., Clement, M.V., and Long, L.H. (2000). Hydrogen Peroxide in the Human Body. FEBS Lett. *486*, 10–13. https://doi.org/10.1016/S0014-5793(00)02197-9.

20. Allen, B.L., Johnson, J.D., and Walker, J.P. (2011). Encapsulation and Enzyme-Mediated Release of Molecular Cargo in Polysulfide Nanoparticles. ACS Nano *5*, 5263–5272. https://doi.org/10.1021/nn201477y.

21. Secret, E., and Andrew, J.S. (2018). Enzyme-Responsive Drug Delivery Systems. In Stimuli-responsive Drug Delivery Systems, A. Singh and M.M. Amiji, eds. (The Royal Society of Chemistry), pp. 209–231. https://doi.org/10.1039/9781788013536-00209.

22. Yoshii, T., Onogi, S., Shigemitsu, H., and Hamachi, I. (2015). Chemically Reactive Supramolecular Hydrogel Coupled with a Signal Amplification System for Enhanced Analyte Sensitivity. J. Am. Chem. Soc. *137*, 3360–3365. https://doi.org/10.1021/ja5131534.

23. Piergentili, I., Hilberath, T., Klemm, B., Hollmann, F., and Eelkema, R. (2023). Enhancing the ROS Sensitivity of a Responsive Supramolecular Hydrogel using Peroxizyme Catalysis. Biomacromolecules *24*, 3184–3192. https://doi.org/10.1021/acs.biomac.3c00262.

24. van der Helm, M.P., Klemm, B., and Eelkema, R. (2019). Organocatalysis in Aqueous Media. Nat. Rev. Chem. *3*, 491–508. https://doi.org/10.1038/s41570-019-0116-0.

25. Bossion, A., Heifferon, K.V., Meabe, L., Zivic, N., Taton, D., Hedrick, J.L., Long, T.E., and Sardon, H. (2019). Opportunities for Organocatalysis in Polymer Synthesis via Step-Growth Methods. Prog. Polym. Sci. *90*, 164–210. https://doi.org/10.1016/j.progpolymsci.2018.11.003.

26. Kiesewetter, M.K., Shin, E.J., Hedrick, J.L., and Waymouth, R.M. (2010). Organocatalysis: Opportunities and Challenges for Polymer Synthesis. Macromolecules *43*, 2093–2107. https://doi.org/10.1021/ma9025948.

27. Kaiho, S., Hmayed, A.A.R., Delle Chiaie, K.R., Worch, J.C., and Dove, A.P. (2022). Designing Thermally Stable Organocatalysts for Poly(ethylene terephthalate) Synthesis: Toward a One-Pot, Closed-Loop Chemical Recycling System for PET. Macromolecules *55*, 10628–10639. https://doi.org/10.1021/acs.macromol.2c01410.

28. Bannin, T.J., and Kiesewetter, M.K. (2015). Poly(thioester) by Organocatalytic Ring-Opening Polymerization. Macromolecules *48*, 5481–5486. https://doi.org/10.1021/acs.macromol.5b01463.

29. Chan, J.M.W., Tan, J.P.K., Engler, A.C., Ke, X., Gao, S., Yang, C., Sardon, H., Yang, Y.Y., and Hedrick, J.L. (2016). Organocatalytic Anticancer Drug Loading of Degradable Polymeric Mixed Micelles via a Biomimetic Mechanism. Macromolecules *49*, 2013–2021. https://doi.org/10.1021/acs.macromol.5b02784.

30. Brinkhuis, R.P., de Graaf, F., Hansen, M.B., Visser, T.R., Rutjes, F.P.J.T., and van Hest, J.C.M. (2013). Dynamically Functionalized Polymersomes via Hydrazone Exchange. Polym. Chem. *4*, 1345–1350. https://doi.org/10.1039/C2PY20789C.

31. de Gracia Lux, C., Joshi-Barr, S., Nguyen, T., Mahmoud, E., Schopf, E., Fomina, N., and Almutairi, A. (2012). Biocompatible Polymeric Nanoparticles Degrade and Release Cargo in Response to Biologically Relevant Levels of Hydrogen Peroxide. J. Am. Chem. Soc. *134*, 15758–15764. https://doi.org/10.1021/ja303372u.

32. Yang, N., Xiao, W., Song, X., Wang, W., and Dong, X. (2020). Recent Advances in Tumor Microenvironment Hydrogen Peroxide-Responsive Materials for Cancer Photodynamic Therapy. Nano-Micro Lett. *12*, 15. https://doi.org/10.1007/s40820-019-0347-0.

33. Iida, H., Imada, Y., and Murahashi, S.I. (2015). Biomimetic Flavin-Catalysed Reactions for Organic Synthesis. Org. Biomol. Chem. *13*, 7599–7613. https://doi.org/10.1039/C5OB00854A.

34. Sakai, T., Kumoi, T., Ishikawa, T., Nitta, T., and Iida, H. (2018). Comparison of Riboflavin-Derived Flavinium Salts Applied to Catalytic H_2O_2 Oxidations. Org. Biomol. Chem. *16*, 3999–4007. https://doi.org/10.1039/C8OB00856F.

35. Minidis, A.B.E., and Bäckvall, J.-E. (2001). Mild and Efficient Flavin-Catalyzed H_2O_2 Oxidations. Chem. Eur J. *7*, 297–302. https://doi.org/10.1002/1521-3765(20010105)7:1<297::AID-CHEM297>3.0.CO;2-6.

36. Ménová, P., Kafka, F., Dvořáková, H., Gunnoo, S., Šanda, M., and Cibulka, R. (2011). Pyrazinium Salts as Efficient Organocatalysts of Mild Oxidations with Hydrogen Peroxide. Adv. Synth. Catal. *353*, 865–870. https://doi.org/10.1002/adsc.201000906.

37. Zhang, S., Li, G., Li, L., Deng, X., Zhao, G., Cui, X., and Tang, Z. (2020). Alloxan-Catalyzed Biomimetic Oxidations with Hydrogen Peroxide or Molecular Oxygen. ACS Catal. *10*, 245–252. https://doi.org/10.1021/acscatal.9b04508.

38. Piergentili, I., Bouwmans, P.R., Reinalda, L., Lewis, R.W., Klemm, B., Liu, H., de Kruijff, R.M., Denkova, A.G., and Eelkema, R. (2022). Thioanisole Ester Based Logic Gate Cascade to Control ROS-Triggered Micellar Degradation. Polym. Chem. *13*, 2383–2390. https://doi.org/10.1039/D2PY00207H.

39. Stingl, K.A., and Tsogoeva, S.B. (2010). Recent Advances in Sulfoxidation Reactions: A Metal-Free Approach. Tetrahedron: Asymmetry *21*, 1055–1074. https://doi.org/10.1016/j.tetasy.2010.05.020.

40. Sato, K., Hyodo, M., Aoki, M., Zheng, X.-Q., and Noyori, R. (2001). Oxidation of Sulfides to Sulfoxides and Sulfones with 30% Hydrogen Peroxide under Organic Solvent- and Halogen-Free Conditions. Tetrahedron *57*, 2469–2476. https://doi.org/10.1016/S0040-4020(01)00068-0.

41. Emmons, W.D. (1957). The Preparation and Properties of Oxaziranes. J. Am. Chem. Soc. *79*, 5739–5754. https://doi.org/10.1021/ja01578a043.

42. Davis, F.A., Lal, S.G., and Durst, H.D. (1988). Chemistry of Oxaziridines. 10. Selective Catalytic Oxidation of Sulfides to Sulfoxides

Using N-sulfonyloxaziridines. J. Org. Chem. *53*, 5004–5007. https://doi.org/10.1021/jo00256a018.

43. Williamson, K.S., Michaelis, D.J., and Yoon, T.P. (2014). Advances in the Chemistry of Oxaziridines. Chem. Rev. *114*, 8016–8036. https://doi.org/10.1021/cr400611n.

44. Schoumacker, S., Hamelin, O., Téti, S., Pécaut, J., and Fontecave, M. (2005). Activation of Oxaziridines by Lewis Acids: Application in Enantioselective Sulfoxidation. J. Org. Chem. *70*, 301–308. https://doi.org/10.1021/jo048380k.

45. DesMarteau, D.D., Petrov, V.A., Montanari, V., Pregnolato, M., and Resnati, G. (1994). Mild and Selective Oxygenation of Sulfides to Sulfoxides and Sulfones by Perfluoro-cis-2,3-dialkyloxaziridines. J. Org. Chem. *59*, 2762–2765. https://doi.org/10.1021/jo00089a020.

46. Page, P.C., Heer, J.P., Bethell, D., Collington, E.W., and Andrews, D.M. (1994). A New System for Catalytic Asymmetric Oxidation of Sulfides Using a Hydrogen Peroxide Based Reagent. Tetrahedron Lett. *35*, 9629–9632. https://doi.org/10.1016/0040-4039(94)88530-3.

47. Bethell, D., Page, P., and Vahedi, H. (2000). Catalytic Asymmetric Oxidation of Sulfides to Sulfoxides Mediated by Chiral 3-Substituted-1,2-benzisothiazole 1,1-Dioxides. J. Org. Chem. *65*, 6756–6760. https://doi.org/10.1021/jo0003100.

48. Cai, M., Xu, K., Li, Y., Nie, Z., Zhang, L., and Luo, S. (2021). Chiral Primary Amine/Ketone Cooperative Catalysis for Asymmetric alpha-Hydroxylation with Hydrogen Peroxide. J. Am. Chem. Soc. *143*, 1078–1087. https://doi.org/10.1021/jacs.0c11787.

49. Kokotos, C., Voutyritsa, E., and Triandafillidi, I. (2016). Green Organocatalytic Oxidation of Sulfides to Sulfoxides and Sulfones. Synthesis *49*, 917–924. https://doi.org/10.1055/s-0036-1588315.

50. Hulea, V., and Moreau, P. (1996). The Solvent Effect in the Sulfoxidation of Thioethers by Hydrogen Peroxide Using Ti-Containing Zeolites as Catalysts. J. Mol. Catal. A: Chem. *113*, 499–505. https://doi.org/10.1016/S1381-1169(96)00273-7.

51. Bhattacharjee, S. (2016). DLS and zeta Potential – What they are and What they are Not? J. Control. Release *235*, 337–351. https://doi.org/10.1016/j.jconrel.2016.06.017.

52. Sobotta, F.H., Kuchenbrod, M.T., Gruschwitz, F.V., Festag, G., Bellstedt, P., Hoeppener, S., and Brendel, J.C. (2021). Tuneable Time Delay in the Burst Release from Oxidation-Sensitive Polymersomes Made by PISA. Angew. Chem. Int. Ed. *60*, 24716–24723. https://doi.org/10.1002/anie.202108928.

53. Fredenberg, S., Wahlgren, M., Reslow, M., and Axelsson, A. (2011). The Mechanisms of Drug Release in Poly(lactic-co-glycolic acid)-based Drug Delivery Systems—A Review. Int. J. Pharm. *415*, 34–52. https://doi.org/10.1016/j.ijpharm.2011.05.049.

54. Pierce, C.J., and Hilinski, M.K. (2014). Chemoselective Hydroxylation of Aliphatic sp^3 C-H Bonds Using a Ketone Catalyst and Aqueous H_2O_2. Org. Lett. *16*, 6504–6507. https://doi.org/10.1021/ol503410e.

55. Triandafillidi, I., Tzaras, D.I., and Kokotos, C.G. (2018). Green Organocatalytic Oxidative Methods using Activated Ketones. ChemCatChem *10*, 2521–2535. https://doi.org/10.1002/cctc.201800013.

56. Ritchie, C.D. (1984). Reactions of .alpha., alpha., alpha.-Trifluoroacetophenone with Nucleophiles in 10:1 Water:Acetonitrile Solution. J. Am. Chem. Soc. *106*, 7187–7194. https://doi.org/10.1021/ja00335a054.

57. Yacob, S., Caulfield, M.J., and Barckholtz, T.A. (2018). Partial Oxidation of Alkanes by Dioxiranes Formed *in situ* at Low Temperature. Philos. Trans. R. Soc., A *376*, 20170055. https://doi.org/10.1098/rsta.2017.0055.

58. Adam, W., Saha-Möller, C.R., and Ganeshpure, P.A. (2001). Synthetic Applications of Nonmetal Catalysts for Homogeneous Oxidations. Chem. Rev. *101*, 3499–3548. https://doi.org/10.1021/cr000019k.

59. Brotzel, F., Chu, Y.C., and Mayr, H. (2007). Nucleophilicities of Primary and Secondary Amines in Water. J. Org. Chem. *72*, 3679–3688. https://doi.org/10.1021/jo062586z.